Distribution and variability of iron input to Oregon coastal waters during the upwelling season

Zanna Chase, Burke Hales, and Timothy Cowles

College of Oceanic and Atmospheric Sciences, Oregon State University, Corvallis, Oregon, USA

Roseanne Schwartz and Alexander van Geen

Lamont Doherty Earth Observatory of Columbia University, Palisades, New York, USA

[1]   We measured iron concentrations off the Oregon coast in spring (May–June) and summer (August) of 2001 as part of the Coastal Ocean Advances in Shelf Transport (COAST) program. Dissolvable and total dissolvable iron levels in surface waters were generally higher in spring (mean of 2.1 and 33.9 nmol L^{-1}, respectively) than in summer (means of 1.4 and 15.4 nmol L^{-1}). In spring and summer, high iron concentrations in surface waters were associated with both cold and saline, recently upwelled waters, and with fresh, relatively warm water influenced by the Columbia River. Comparison of total dissolvable iron in 0.45 μm filtered and in unfiltered samples indicated a substantial contribution from particulate iron. Iron concentrations in summer were generally lower than in spring throughout the water column, with the exception of the near-bottom, where concentrations were generally higher in summer than spring. Optical backscatter data from moored sensors were used to infer the vertical and cross-shelf transport of iron-bearing particles during the upwelling season over a steep shelf. Cross-correlation analysis showed downslope movement of particles from the deep inner shelf to the deep midshelf. There was also evidence for sinking of biogenic particles at the midshelf and inner shelf, but we found no evidence of upslope transport of benthic particles. Sufficient iron is available in this system to meet the demands of the phytoplankton, which are able to make full use of available nitrate.

1.   Introduction

[2]   Years ago, *Gran* [1931, p. 41] noted the greater abundance of phytoplankton in the coastal ocean and hypothesized that this was due to "iron-containing humus-compounds drained out from land." Iron is an essential micro-nutrient with very different chemical behavior than the macro-nutrients. In the coastal zone iron is supplied by sediment resuspension, rivers, wind-borne dust and mixing or upwelling of deep waters. This is in contrast to the macro-nutrients, which in the absence of anthropogenic impacts are supplied primarily by mixing from deep waters and to some extent by rivers. To a greater degree than the macro-nutrients, iron exists in multiple chemical and physical forms in the coastal ocean. These include dissolved inorganic iron, organically complexed iron, particulate iron (>0.2 μm), colloidal iron (1–1000 nm) and reduced iron (Fe^{2+}). All of these forms are most likely available to phytoplankton but over different timescales [*Bruland and Rue*, 2001].

[3]   The proximity to iron sources in coastal regions led to the assumption that iron was always in abundance in these waters, in contrast to the open ocean, where iron limitation is common [e.g., *Fung et al.*, 2000]. Closer examination of the central California upwelling system, however, revealed signs of iron control of phytoplankton production and community composition [*Bruland et al.*, 2001; *Hutchins and Bruland*, 1998; *Johnson et al.*, 2001]. This unexpected coastal iron limitation appears to arise from a combination of upwelling circulation, which supplies ample macro-nutrients, persistent alongshore rather than cross-shore winds, minimal summertime river runoff and a narrow continental shelf. Iron availability in the coastal ocean has been linked to the release of toxic domoic acid by the diatom *Pseudo-nitzschia* [*Maldonado et al.*, 2002], to the presence of *Trichodesmium* [*Lenes et al.*, 2001], and to the contrast in productivity between the Oregon and Washington coasts [*Hickey and Banas*, 2003].

[4]   As part of the Coastal Ocean Advances in Shelf Transport (COAST) project we measured iron concentrations in surface waters and in vertical profiles off the Oregon coast during the spring (May–June) and summer (August) of 2001. The goal was to better understand the seasonal progression of iron supply in regions of "simple" (steep) and "complex" (shallow) topography. Modeling work [*Allen et al.*, 1995] has shown that when upwelling

occurs over a shallow shelf it is more concentrated within the bottom boundary layer than when it occurs over a steep shelf. This should have consequences for iron supply. Further insight into iron dynamics was obtained by mounting backscatter meters at the surface and near the bottom of two moorings deployed for the whole summer at the site with simple topography. By monitoring the abundance of particles near the surface and near the bottom we hoped to be able to track the movement of iron-bearing particles across the shelf.

2. Methods

2.1. Chemical Measurements

[5] Iron was sampled from the R/V *Wecoma* during two 3 week cruises in the summer of 2001: survey 1, 23 May–16 June and survey 2, 6–26 August. These cruises involved extensive mapping with a SeaSoar, with the aim of capturing repeated near-synoptic descriptions of the entire study area. Surface water iron concentrations were mapped throughout the SeaSoar operations with an underway flow injection analysis (FIA) system, described below. In addition, a total of 15 profiles were analyzed for Fe (eight from survey 1 and seven from survey 2).

[6] Sample collection and analysis was slightly modified from the system described by *Chase et al.* [2002]. A continuous supply of near-surface (0–5 m) water was peristaltically pumped into the laboratory through acid-cleaned silicone and teflon-lined polyethylene tubing attached to a brass "fish" [*Vink et al.*, 2000]. The fish was deployed off a 5 foot boom on the starboard side. The sample stream passed through a 20 μm acid-cleaned capsule filter followed by a ~30 s in-line acidification to pH 3.3 ± 0.1 before entering the FIA manifold, unlike *Chase et al.* [2002], where neither filtration nor acidification was employed. The coarse filtration was added to avoid clogging valves with large particles. Acidification was added to make the method comparable to the operationally defined "dissolvable iron" measured by others [*Fitzwater et al.*, 2003; *Johnson et al.*, 2001]. Iron was detected following the method of *Measures et al.* [1995] without preconcentration, and using a 6 cm flow cell. Standards were prepared in acidified low-iron seawater and were run at least every 5 hours and whenever new reagents were prepared. The detection limit ranged from 0.3 to 0.7 nmol L^{-1}. A system blank was assessed by injecting carrier (pH 3 milli-Q water) as a sample. The blank associated with sample acidification was determined by making double the addition of acid, and was found to be below detection. The cleanliness of the surface pumping system was checked by collecting several surface samples directly into a clean 1 L bottle while underway. The bottle was lowered to the surface by a clean line tied around its neck. Iron concentrations were the same as those collected simultaneously from the pumping system (10.9 ± 0.2 and 11.1 ± 0.3 in the pumping system and discrete sample, respectively).

[7] The underway analysis result in an operationally defined measurement of iron; it does not quantitatively recover colloidal iron or iron bound to strong organic ligands, and the fraction released from particles is also operational. In the manuscript we refer to this fraction as dissolvable iron (dFe).

[8] Additional samples were stored in hot-acid-leached (1.2N HCl at 60°C for 24 hours) LDPE bottles for later analysis. These bottle samples included water collected from the surface pumping system (also filtered through the 20 μm filter) as well as water collected from a conductivity-temperature-depth (CTD) Rosette (not filtered unless otherwise specified). Niskin bottles were modified for trace metal work [*Chase et al.*, 2002] and acid leached (1.2N HCl for 24 hours) prior to sampling. The Rosette was deployed on standard hydrowire. A subset of the profile samples was filtered by peristaltically pumping through acid-clean 0.45 μm syringe filters (Millipore) to give dissolved iron. All bottle samples were stored in the dark with 2 ml L^{-1} concentrated HCl for 24–28 months before being analyzed using a modified version of the FIA system that was used at sea. In this case the pH of the carrier and standards was changed to match the pH (~1.8) of the samples. Because many of the acidified unfiltered samples had very high iron concentrations, we ran samples with over 25 nmol L^{-1} using a 2 cm flow cell. With this configuration the system was linear to 200 nmol L^{-1}. Samples with concentrations greater than the linear range were diluted with low-iron seawater. Replicate analyses of high iron (5–50 nmol L^{-1}) samples on different days agreed within 2–3%, while replicate analyses of lower-iron (1–5 nmol L^{-1}) samples on different days agreed within 5–10%. Analysis of CASS-4 (National Research Council of Canada) on multiple days showed good agreement with the certified value (14 ± 1 nmol L^{-1}, measured; 13 ± 1 nmol L^{-1}, certified value).

[9] The unfiltered discrete samples represent another operationally defined measurement. The fraction measured includes iron desorbed from particles under storage at pH 1.8 for more than 12 months. We call this fraction "total dissolvable iron (TdFe)." Several samples run after both 12 and 24 months storage showed no significant trend due to storage.

[10] Nutrient samples were collected directly from the CTD Rosette (i.e., not filtered) and stored frozen. They were analyzed by a modification of standard colorimetric methods [*Gordon et al.*, 1994].

2.2. Particle Concentration From Moorings

[11] Volume scattering function (VSF) meters (model ECO-VSFSB from WetLabs) were deployed at 15 m below the surface at all COAST moorings (see Levine et al., Horizontal circulation and momentum balance off the Oregon coast: Moored observations during summer 2001, submitted to *Journal of Geophysical Research*, 2004, hereinafter referred to as Levine et al., submitted manuscript, 2004). The instruments detect backscatter at three angles (100°, 125° and 150°) and one wavelength (440 nm). At the inner shelf and midshelf sites along 45°N (CH line), additional backscatter meters were deployed 15 m above the bottom. The deep sensors sampled every 1.25 hours while those near the surface sampled every 0.5 hours. The backscattering coefficient due to particles (Bbp (m^{-1})) was calculated from the VSF measured at the three angles after subtracting the contribution from water at each angle [*Boss and Pegau*, 2001]. Optical backscatter is highly sensitive to particle size, with particles <20 μm being much more efficient in scattering [*Bunt et al.*, 1999]. Thus we tracked

Table 1. Median Value of Bottom Depth, Sea Surface Temperature (SST), and Surface Salinity for All Measurements Along the Cruise Tracks in Spring and Summer Compared to the Values Colocated With Underway and Discrete Iron Measurements

	Bottom Depth, m		SST, °C		Salinity	
	Spring	Summer	Spring	Summer	Spring	Summer
Underway Fe	126.2	115.3	13.53	13.88	31.40	32.48
Discrete Fe	117.9	110.8	12.65	13.93	31.20	32.36
All underway data	113.4	125.9	13.08	14.14	31.00	32.35

fine-grained particles in particular. Data were interpolated to a common (lower-resolution) time and then smoothed with a four-point running mean prior to further analysis. Correlations between the Bbp values at different locations were calculated for a range of lag times (described further in section 4.2) using the "corrcoef" function in Matlab.

3. Results

3.1. Surface Concentrations

[12] The distribution of iron in surface waters was quantified both at sea, with underway mapping, and from discrete samples collected underway and analyzed at LDEO. Discrete surface samples were collected throughout both cruises every 1–3 hours. We attempted to operate the underway system during all SeaSoar operations. However, significant data gaps arose due to equipment failure. The longest gap occurred the first 8 days of the August cruise (7–15 August) but other shorter gaps occurred throughout the cruises. The SeaSoar completed five near-synoptic surveys of the study area during each cruise [*Castelao and Barth*, 2005]. Because of the gaps in the underway data and the relatively sparse sampling of the discrete samples we were unable to produce meaningful synoptic

maps of iron distributions in surface waters, similar to those produced for other variables such as temperature. Instead we focus here on broad patterns observed when all of the data for each cruise are pooled together.

[13] In order to compare these "composite" distributions we need to identify potential bias that may arise because the discrete and underway samples were collected at different times and locations and not necessarily along a regular grid. For example, it may be that the underway data were only collected during calm periods. We evaluate this possibility by examining median values of bottom depth, surface salinity and surface temperature associated with underway samples, discrete samples and the complete ship's underway data stream (Table 1). In general discrete and underway samples appear to have been collected at representative times, without obvious bias. The spring underway samples are from slightly deeper and warmer water than average surface water sampled by the ship's intake.

[14] Concentrations of both dFe (Figure 1) and TdFe (Figure 2) in surface waters are higher in spring than summer (Table 2). The difference between spring and summer is more apparent in the TdFe data, and south of 44.5°N (Table 2). Total dissolvable Fe concentrations are roughly an order of magnitude greater than dFe concentrations. In spring a "plume" of high TdFe is observed extending seaward from 44.5°N (Figure 2). This plume is not present in August and is seen only weakly in the dFe data. During both seasons higher concentrations of TdFe and dFe are found in the north than the south of the study area with the contrast being greater for TdFe (Table 2).

[15] Dissolvable iron is highest in cold, salty water in spring, but is also consistently greater than 2 nmol L^{-1} in waters with salinity <30 (Figure 3). Cold, salty surface waters are also relatively rich in dFe in summer (though less so than in spring), with the highest dFe values found at moderate salinity and temperature (Figure 3). Total dissolvable Fe is
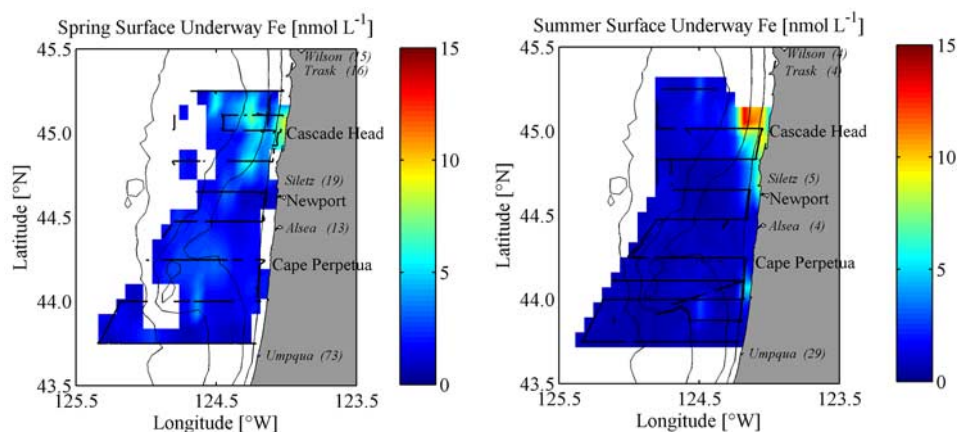

Figure 1. Near-surface iron concentrations measured underway (dissolvable Fe) in spring and summer 2001. The largest rivers of this area are indicated in italics, with their flow during spring (May and June) and summer (July and August) of 2001 indicted in parentheses (m^3/s). Data are from the U.S. Geological Survey. The flow from the largest coast river, the Umpqua, is in both seasons close to 100 times smaller than the flow from the Columbia River. Iron contouring was achieved using a distance-weighted running average procedure available with the software package Surfer (Golden Software). The contour interval is 5 km in longitude and 10 km in latitude. Bathymetric contours are drawn for 50 m, 100 m, 200 m, and 1000 m.
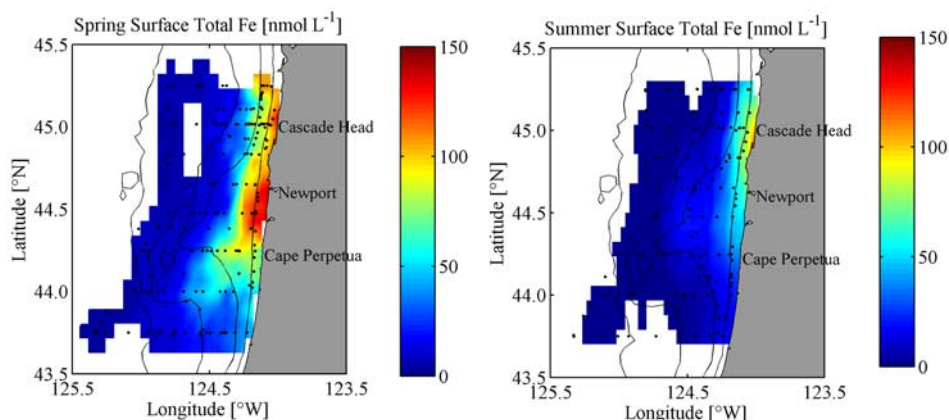
Figure 2. Same as Figure 1, but for discrete samples collected from the clean pumping system, stored acidified at pH $\sim$ 1.8 and analyzed 24–28 months later.

generally highest in the warmest and saltiest waters in both seasons (Figure 3).

3.2. Profiles

[16] Vertical profiles of iron concentration were determined at six stations corresponding to the locations of COAST moorings (Levine et al., submitted manuscript, 2004) along the Cascade Head (CH) (45°N) and Cape Perpetua (CP) (44.22°N) lines. The stations along each line were chosen to represent the inner shelf, the midshelf and the shelf break; though the distance of the stations from shore differs between the two lines (being closer to shore along the CH line), they have similar bottom depths. As expected, TdFe concentrations are lowest at the shelf break and increase toward shore (Figure 4). Iron concentrations are higher along the CH line when comparing stations at similar times and bottom depths, with the exception of June at the midshelf. In most cases TdFe concentrations in summer are less than or equal to those in spring at all depths except the deepest, where concentrations are generally higher in summer (Figure 4).

[17] Profiles CP-2 and CP-4 show evidence of significant loss of TdFe between 2 and 10 June (Figure 4). The second of June was a period of strong upwelling, while by 10 June winds had relaxed considerably and upwelling was minimal [*Castelao and Barth*, 2005]. The difference in the two profiles may therefore be the result of particulate Fe settling from the water column during the period of calm.

[18] The 0.45 μm filtered samples contain substantially less iron than unfiltered samples (Figure 5); on average the iron concentration in filtered samples is 25 times lower than in unfiltered samples. Dissolved iron concentrations are 0.8–4 nmol L^{-1} in surface waters, increasing to 6–17 nmol L^{-1} in the near-bottom samples. The available profiles show less north-south and June–August differentiation in the

filtered samples, relative to the unfiltered samples. Iron concentrations in filtered and unfiltered samples are significantly correlated ($r = 0.58$; $n = 58$, $p < 0.005$). This average correlation encompasses a weak and nonsignificant correlation on the CH line and a strong, significant correlation on the CP line ($r = 0.79$; $n = 38$, $p < 0.005$).

[19] Nitrate profiles at the same stations serve as a macronutrient contrast to the iron profiles (Figure 6). Nitrate concentrations are in general higher along the CP line than the CH line. With the exception of the CP inner shelf site, and away from the bottom, nitrate concentrations are higher in summer than in spring (Figure 6). Both observations are in contrast to the situation for iron.

3.3. Particle Concentrations

[20] The percent transmission, measured with a transmissometer on the CTD-Rosette, varies between 90 and about 60% at the stations corresponding to the mooring locations (Figure 7). All profiles show a decrease in light transmission toward the bottom, indicating a greater concentration of particles. At the inner and midshelf, light transmission at the surface and near the bottom is generally less at the southern (CP) line than the northern (CH) line.

[21] All four backscatter sensors on the CH line moorings collected data throughout the upwelling season with no signs of fouling (Figure 8). Particle concentrations at all four sites vary within roughly the same range, and show similar patterns of variability. The limited number of transmissometry profiles at the mooring locations indicate at least qualitative agreement with the backscatter data. On 7 June, for example, both the transmissometry and the backscatter show higher particle concentrations at 15 m from the surface than 15 m from the bottom, with the difference more pronounced at the inner shelf than the midshelf. Matching up the backscatter reading at the mooring with

Table 2. Mean Values of Underway and Discrete Iron in Surface Waters, Calculated From Gridded Fields[a]

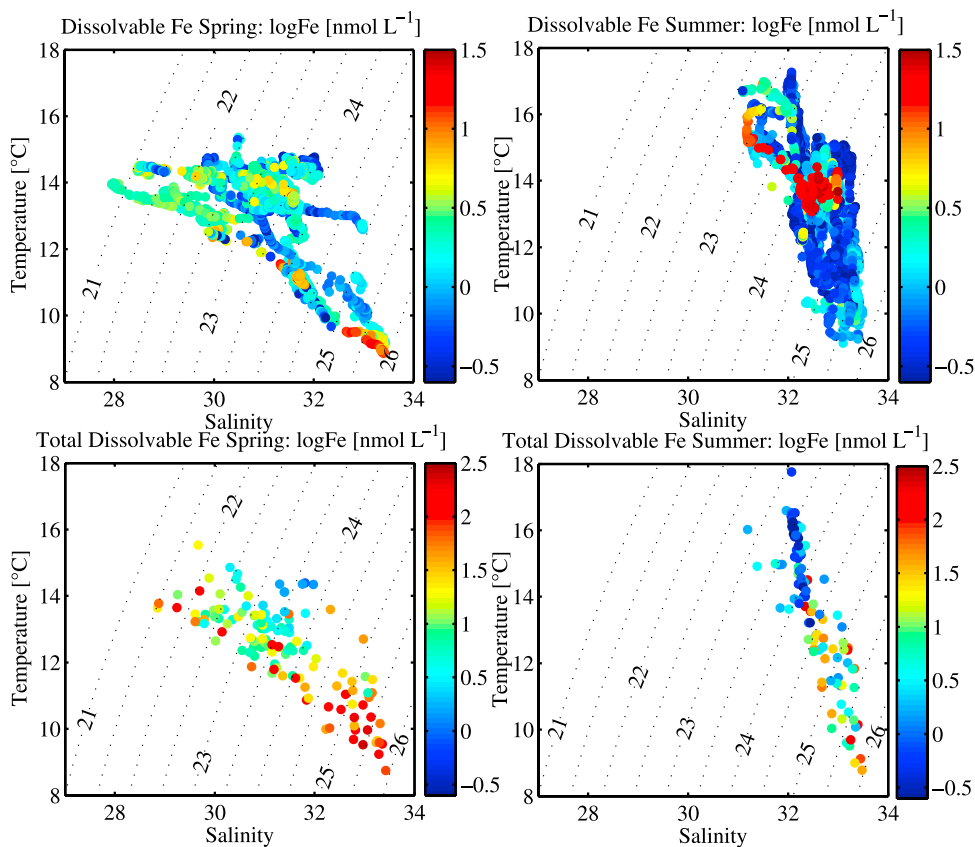|	All Data		North of 44.5°N		South of 44.5°N	
	Spring	Summer	Spring	Summer	Spring	Summer
Underway (dFe), nmol L^{-1}	2.1	1.4	2.6	2.4	1.7	0.8
Discrete (TdFe), nmol L^{-1}	33.9	15.4	35.9	21.6	32.5	10.4

[a]Figures 1 and 2.

Figure 3. Dissolvable (underway) and total dissolvable (discrete) near-surface iron concentrations in temperature-salinity space. Lines of constant density (sigma-0) are indicated in each case. Note the logarithmic scale used for Fe and the different color scale for dFe and TdFe.

the transmissometry from a nearby CTD (10 samples total, 2×2 depths at CH3 and 3×2 depths at CH2) shows a rough negative correlation (data not shown); the lowest backscatter (0.003) corresponds to the highest transmission (89.7%) and the highest backscatter (0.0124) corresponds to the lowest transmission (84.1%). Insufficient data are available for a more rigorous comparison.

4. Discussion

[22] The two main observations from this work are that iron concentrations in surface waters are generally higher north of 44.5°N than to the south, and that iron concentrations in surface waters are generally lower in summer than in spring. In the following we discuss the factors that contribute to these spatial and temporal trends in iron on the Oregon coast.

4.1. River Input

[23] During summer the Columbia River plume extends south of the river mouth (near 46.25°N) into the region studied by COAST. The influence of the Columbia River, identified by salinity less than 32.5 [*Huyer et al.*, 2002] is clearly visible in our study area, particularly in spring (e.g., Figure 3) and particularly in the north [*Castelao and Barth*, 2005]. The dissolved iron (<0.45 μm) concentration in the Columbia River proper is about $0.1-1$ μmol L^{-1} [*Fuhrer et al.*, 1996] and even in the ocean the river plume is rich in

iron [*Lohan and Bruland*, 2004]. In July 1999, a year in which flow was roughly twice what it was in 2001, surface waters with salinity <29 were found offshore at 44.6°N, where TdFe was $14-74$ nmol L^{-1} and dFe between 5 and 10 nmol L^{-1} [*Chase et al.*, 2002]. In the 2001 data the association between high iron and low salinity is not as apparent as it was in 1999, perhaps due to the lower flow from the Columbia in 2001. Nevertheless, in spring, the low-salinity waters generally have dFe concentrations of between 1.5 and 5 nmol L^{-1} (Figure 3). The flow from the Columbia is reduced in summer relative to spring, and this is reflected in higher average surface salinity in summer [*Castelao and Barth*, 2005]. Given that the plume is rich in iron, its reduced presence in summer may contribute to the generally lower surface water iron concentrations in summer, particularly away from the very near shore, which is most influenced by resuspension and upwelling.

[24] Quantifying the effect of reduced river flow on iron distributions is difficult. The flow decreased by 40% between May–June and August (based on data from the U.S. Geological Survey [*Castelao and Barth*, 2005]). However, because the Columbia does not discharge directly into the COAST site, the amount of river water reaching the site is affected not only by the discharge but also by the trajectory of the plume, which varies with upwelling intensity. The average of all underway surface salinity measurements is 31.1 in spring and 32.4 in summer, an increase of only 4%. Thus the seasonal changes in river flow (40% decrease) are
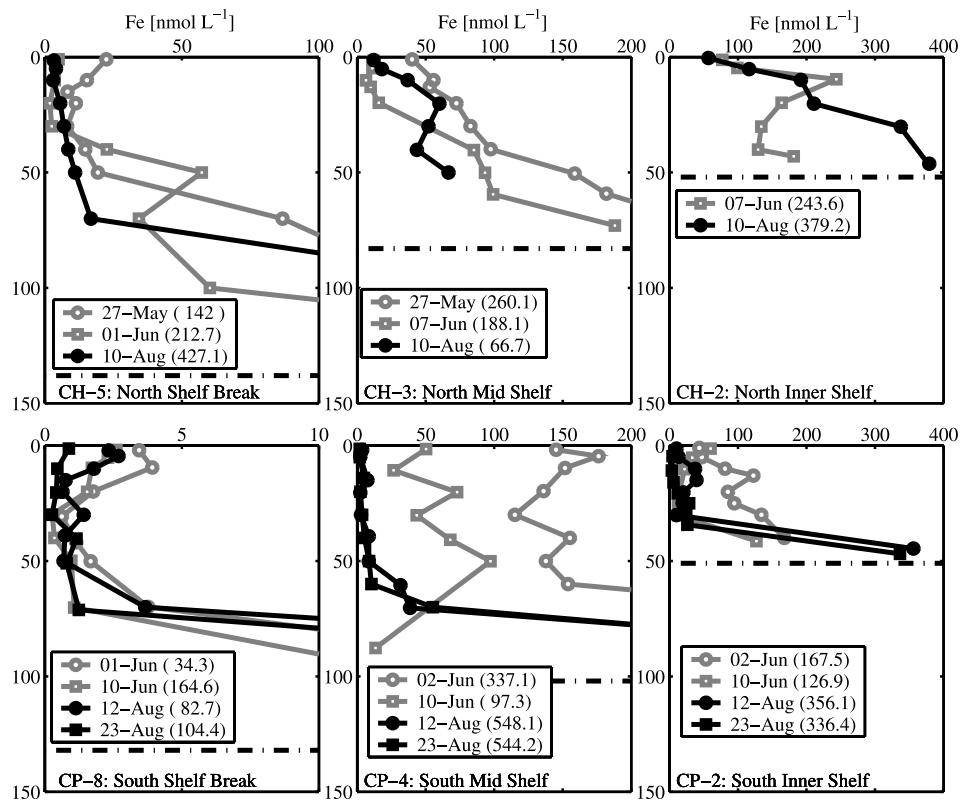
Figure 4. Profiles of total dissolvable iron along the Cascade Head (45°N) (CH) and Cape Perpetua (44.22°N) (CP) lines. The stations are approximately 6, 10, and 18 km from shore along the CH line and 6, 29, and 64 km from shore along the CP line. These stations correspond roughly to the locations of the Coastal Ocean Advances in Shelf Transport (COAST) moorings (Levine et al., submitted manuscript, 2004). Different x axis scales are used. In some cases, high iron values are off the scale. The highest iron value in the profile is noted in parentheses next to the date in the legend.

dampened by the time the signal is expressed in the COAST region. Furthermore, salinity alone cannot be used to constrain the relative presence of river water, since an increase in upwelling will also produce higher surface salinity. Surface waters can be considered a mixture of a minimum of three fractions: Columbia River water, upwelled water and offshore water. A minimum of three near-conservative tracers with distinct signatures in these three fractions is therefore needed in order to constrain the magnitude of these fractions in each season. Unfortunately the required tracers are not available here. A more comprehensive budgeting of Columbia River influence on the Oregon coast in summer awaits a study combining iron concentrations in surface water source regions with measurement of conservative tracers in these water masses.

4.2. Particle Dynamics

[25] Particulate iron is clearly an important contributor to total iron in this region (e.g., compare Figures 1 and 2 and Figures 4 and 6). Furthermore, TdFe, which includes a fraction of particulate iron, shows a larger decrease between summer and spring than does dFe, and a larger differentiation north and south of 44.5°N (Table 2). Working north of Monterey Bay, California, *Fitzwater et al.* [2003] observed high concentrations of particulate Fe (17.7–359 nmol Kg^{-1}) in upwelling plumes. They also found suspended particulate material (SPM) within the plumes was signifi-

cantly more iron-rich than SPM outside the plume. These observations suggest the supply of particulate iron is central to understanding many of the features of the iron distributions in coastal upwelling systems.

[26] One of the classic views of upwelling circulation is of a "conveyor," where a parcel of water is thought to follow a path from near the bottom at midshelf, shoreward and up the slope, then to the surface, and finally moving offshore in the surface Ekman layer [e.g., *Smith et al.*, 1983]. Such a route from near-bottom to surface could be an important means of transporting particulate Fe to the surface. Indeed, the far-onshore extension of the upwelling cell was recently confirmed by shore-based sampling off Oregon [*Takesue and van Geen*, 2002; *van Geen et al.*, 2000]. A detailed study of the dynamics of the bottom boundary layer along the CH line [*Perlin et al.*, 2005] has documented increased turbulence during wind relaxation, synchronous with the mobilization of fine sediments. Up-slope movement of dense, turbid bottom water then occurs during upwelling [*Perlin et al.*, 2005]. Particle-rich water in such close contact with the shelf should be rich in iron. Seasonal changes in these processes may impact the amount of particulate iron mobilized from shelf sediments.

[27] We used the time series of optical backscatter data to investigate particle dynamics on the shelf (midshelf and inner shelf at 45°N). We were specifically interested in evidence of shelf particles being transported up the slope
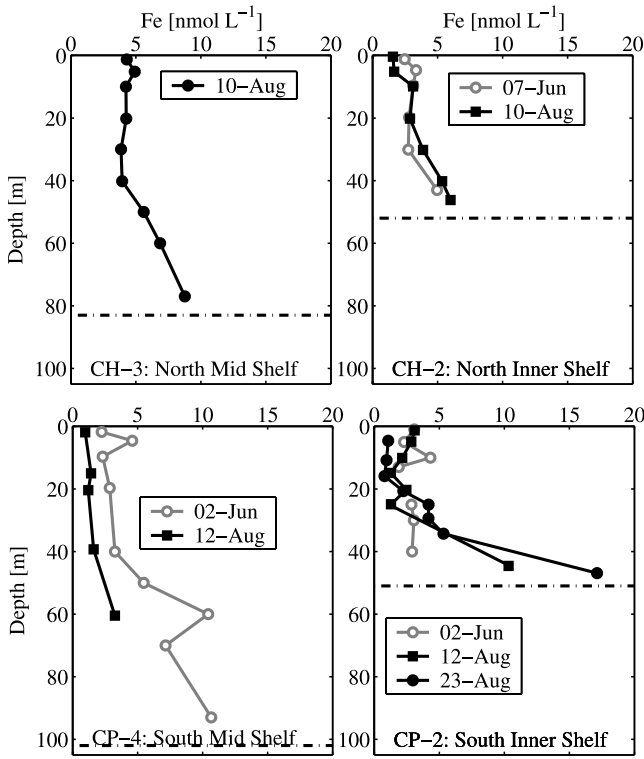
Figure 5. Same as Figure 4, but for dissolved Fe (<0.45 μm).

and eventually into the surface and offshore, i.e., following the conveyor. Lagged cross correlations were used to elucidate particle dynamics. The reasoning was that if the conveyor holds for particles, then, for example, particle concentrations on the inner shelf at depth should be well correlated, after a lag for transport, with particle concentrations on the midshelf at depth. Likewise for particle concentrations at the surface on the inner shelf and at depth. Using the entire mooring record (Figure 8) we calculated the correlation between different pairs of backscatter measurements on the moorings at lag periods up to 4 days (Figure 9). The results are more readily interpreted in schematic form where the maximum correlation and corresponding lag are shown together with arrows indicating the sense of the lag (Figure 10). Obvious features from this analysis are: (1) particle concentrations at the inner and midshelf are highly correlated with a lag time close to zero and (2) at the inner and midshelf, particle concentrations near the surface are correlated with particle concentrations near the bottom, with a lag of half a day at the inner shelf and about 3 days at the midshelf and (3) there is no evidence of particles moving upslope and into the surface along the "conveyor."

[28] The strong zero-lag correlations between mid- and inner shelf may arise either because particle supply via sinking (deep sites), biogenic production (surface sites) and resuspension occurs simultaneously at the two sites, or because there is very rapid transport of particles between
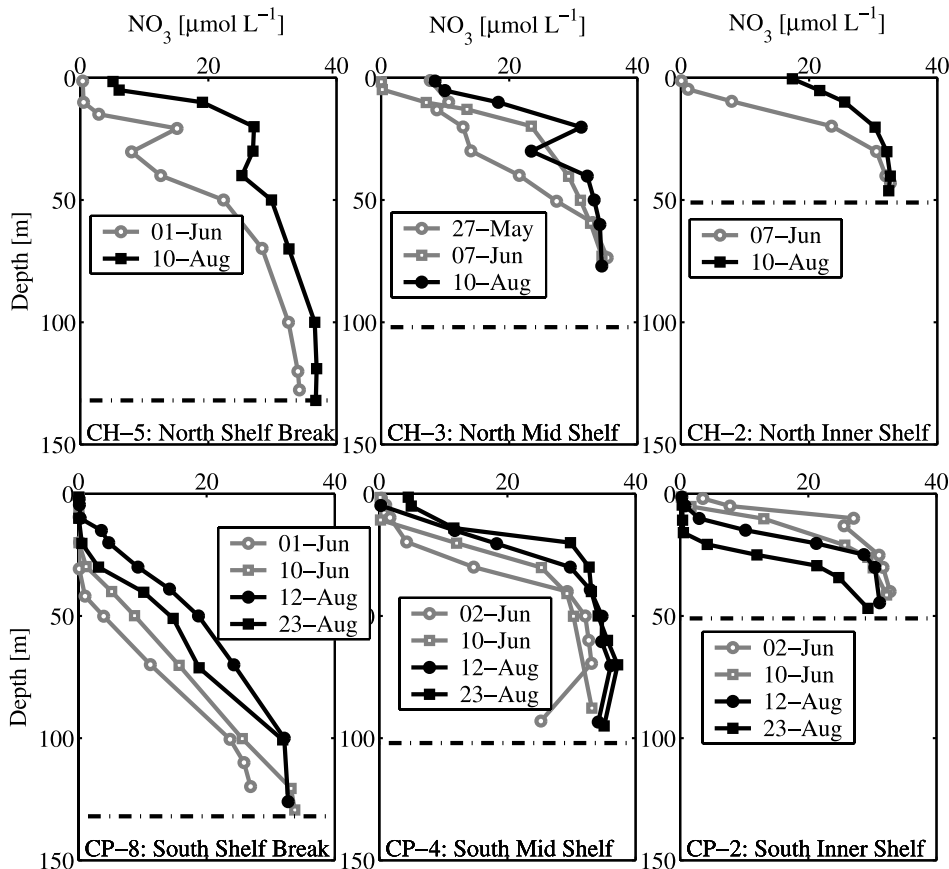

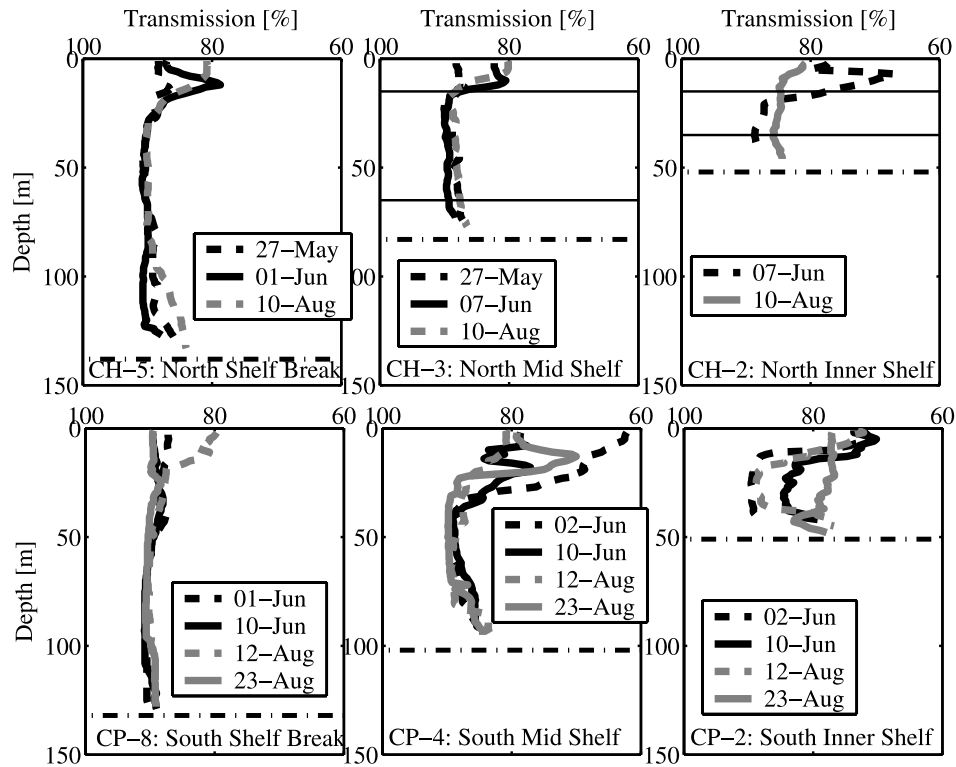**Figure 6.** Same as Figure 4, but for nitrate.

Figure 7. Same as Figure 4, but for light transmission. The *x* axis scale is inverted so that particle concentration increases to the left with decreasing light transmission. The solid horizontal lines in panels for CH-3 and CH-2 correspond to the depth of the backscatter sensors deployed at these two stations as discussed in the text.
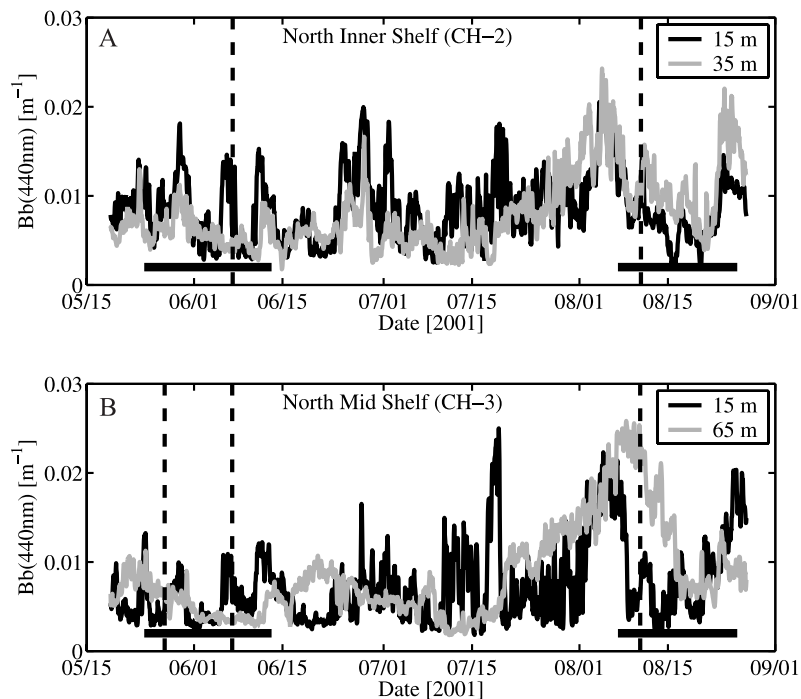

Figure 8. Volume backscatter at 440 nm, a proxy for particle concentration, at the northern mooring line (CH). (a) Inner shelf and (b) midshelf locations each had a sensor at 15 m below the surface and 15 m above the bottom. Horizontal lines indicate the times of the two survey cruises. Data have been smoothed with a four-point (5 hour) running mean.
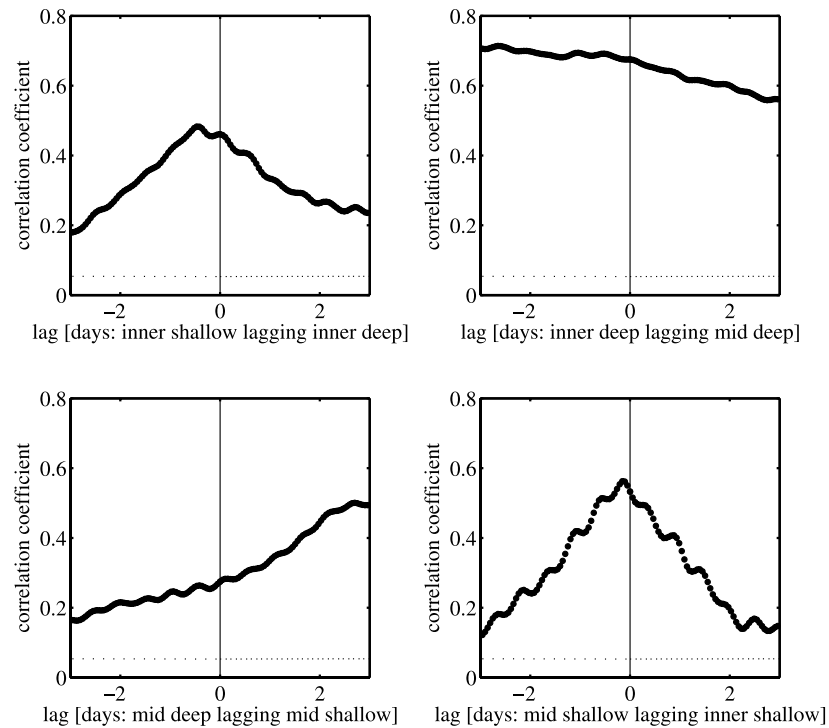
Figure 9. Lagged cross-correlation analysis of four combinations of the backscatter data in Figure 8. The correlation between two time series is shown as a function of the lag between the time series. Near-horizontal lines bracket values of the correlation coefficient that are not significantly different from zero ($p = 0.001$).

the inner and the midshelf. The trend toward a positive lag at depth between the mid- and the inner shelf (Figure 10) suggests that at least at depth, there is some element of downslope particle transport.

[29] The weaker, yet statistically significant, lagged correlations between particle concentrations near the surface and near the bottom at both the inner and the midshelf is consistent with sinking of particles. At the inner shelf the lag is short, close to half a day, whereas at the midshelf, the maximum correlation corresponds to a lag of close to 3 days. These lag times imply sinking rates of 40 m d^{-1} and 17 m d^{-1} at the inner and midshelf, respectively. These sinking particles are most likely biogenic particles produced at the surface in response to nutrient and iron supply. Fluorometers were deployed together with the backscatter meters at 15 m below the surface. Chlorophyll and backscatter were highly correlated at the midshelf and inner shelf sites ($r^2 = 0.82$ and 0.69, respectively; $n = 1933$, $p < 0.005$). The implied sinking rates, however, are too fast to be intact phytoplankton cells. According to Stoke's law, spherical diatoms with a density of 1100 g kg^{-1} [*van Ierland and Peperzak*, 1984], would have to be 200 and 43 μm in diameter at the inner and midshelf, respectively, to achieve the inferred sinking rates. These sizes are pushing the limit of realistic sizes for coastal phytoplankton. Aggregates of cells and clay particles [*Hamm*, 2002], however, could achieve fast sinking rates at the smaller sizes that preferentially contribute to optical backscatter [*Bunt et al.*, 1999].

[30] In summary, the moored particle sensors do not show evidence of a conveyor of particles up the slope and offshore. If anything, they show downslope movement of particles. It is

still possible that upslope movement occurs [*Perlin et al.*, 2005], but is restricted to a depth range closer to the bottom and was missed by our placement of the deep sensor.

[31] The backscatter sensors do show evidence of export of biogenic particles from the surface, at both the midshelf and the inner shelf. This is consistent with the observation
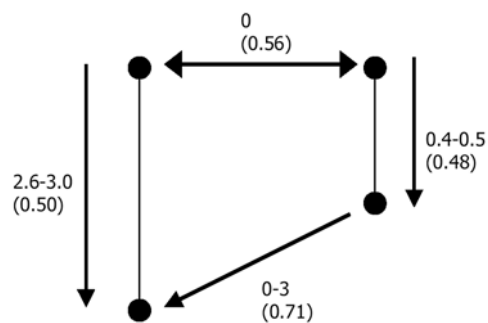

Figure 10. Schematic of the results shown in Figure 9. Black circles represent the locations of the four backscatter sensors: two on the inner shelf and two on the midshelf. Numbers on top indicate the lag in days giving the maximum correlation between pairs of sensors joined by arrows. Numbers in parentheses are the correlation coefficients. For example, Bb from the deep sensor on the midshelf lags that from the shallow sensor on the midshelf by 2.6–3.0 days, at which point the correlation between the two series is $r = 0.50$. Total number of observations per correlation is between 1875 and 1933.

that a substantial portion of shelf productivity is exported off the shelf each season [*Hales et al.*, 2003]. Because POC concentrations were roughly equivalent in spring and summer (P. Wheeler, unpublished data, 2001), increased biological activity [*Castelao and Barth*, 2005] cannot readily account for the lower iron concentrations in summer via partitioning to the particulate phase. It is possible, however, that continued growth through the summer acts to progressively export phytoplankton-associated iron from the shelf, so that by the end of the summer the *total* inventory of iron on the shelf is substantially less than in spring. The water column profiles (e.g., Figure 4) confirm this idea to some extent, in that iron concentrations in summer are generally lower throughout the water column, and not just at the surface. However, there is evidence of elevated iron concentrations in August near the bottom, particularly on the inner shelf at Cape Perpetua (Figure 5); it may be that in late summer surface iron is simply "trapped" in an iron-rich layer near the bottom. These elevated near-bottom dissolved iron values may also result from a larger flux of dissolved iron from the sediment [*Berelson et al.*, 2003; *Elrod et al.*, 2004] during late summer. Sampling with more complete depth coverage, including the sediment, would be needed to test the idea of substantial summertime iron export from the shelf or trapping in the bottom boundary layer.

[32] Because shelf sediments are an important source of iron to coastal surface waters [*Johnson et al.*, 1999], shelf width has been identified as a key variable regulating iron supply to coastal upwelling systems [*Bruland et al.*, 2001; *Chase et al.*, 2005]. This may partly be due to the fact that upwelling over a wide, shallow shelf occurs, in models, to a greater extent in the bottom boundary layer, as opposed to in the interior [*Allen et al.*, 1995]. Upwelling through the bottom boundary layer should afford greater contact with iron-rich sediments and benthic dissolved iron [*Berelson et al.*, 2003; *Elrod et al.*, 2004]. In the COAST region higher nearshore iron concentrations are found in the north, the area with the narrower, steeper shelf (this is particularly evident in summer; see Figures 1 and 2). However, the shelf in the COAST study area is in general wider than that off central California. If we define the shelf width as the distance to the 150 m isobath, even the "narrow" shelf at the CH line is twice as wide as the "wide" shelf north of Monterey Bay studied previously [*Bruland et al.*, 2001; *Chase et al.*, 2005]. Thus there may be a minimum critical shelf width beyond which further increases in shelf width do not significantly affect iron supply. Alternatively, other factors such as the presence of the Columbia River to the north, the inshore intrusion of offshore waters south of Heceta Bank, or sediment composition, may obscure the effect of shelf width in this region.

[33] The type of sediment is another variable that might affect the degree of remobilization and supply to the surface. Sandy sediments cover most of the nearshore bottom in the northern part of our study area down to the southern end of Heceta Bank (e.g., from 46° to 44°N), with the region further south being a mixture of muddy sand and mud [*Kulm et al.*, 1975]. Thus sandy sediments are beneath the region of higher surface iron, and muddy sediments beneath the region with low iron. This association may be completely coincidental; although high iron fluxes have been documented from muddy shelf sediments [*Berelson*

et al., 2003], very little is known of the geochemical reactivity of sandy sediments (but metal fluxes may be high [*Huettel et al.*, 1998]). At the same time, the finer sediment to the south indicates a depositional area, and hence less particle resuspension. In summary, sediment type is poorly characterized in this region, but grain size does roughly correlate with surface iron, and the simplest explanation is that the finer grained sediment corresponds to a region of reduced sediment resuspension.

4.3. Circulation Effects

[34] Differences in upwelling strength during spring and summer may contribute to the difference in mean iron concentrations. A convenient measure of upwelling intensity is given by the integral of the wind stress over a 5 day timescale, (W_{5d}), as defined by *Castelao and Barth* [2005]. Using this measure calculated from the winds at NDBC buoy 46050 at Stonewall Bank, we find significant differences in the distribution of upwelling conditions *during iron sampling* in spring and summer (Figures 11a and 11b). Specifically, the mean W_{5d} is lower (more upwelling-favorable) in spring (-8.9) than in summer (-6.8) whereas the median W_{5d} is lower in summer (-12) than in spring (-4.1). That is, there were a few episodes of intense upwelling in spring, but more persistent moderate upwelling in summer. The impact of these differences in upwelling on iron concentrations is difficult to assess. From the corresponding surface dFe concentrations (Figures 11c and 11d) it appears that large iron inputs are associated with both strong upwelling ($W_{5d} < 10$) and strong downwelling conditions ($W_{5d} > 10$). However, the considerable spatial variability in iron measurements that is contained in Figure 11 makes it difficult to isolate the effect of upwelling. More time series observations are needed to fully understand the link between upwelling, downwelling and iron input at a given location.

[35] In their study of the seasonal cycle of iron in surface waters in Monterey Bay, California, *Johnson et al.* [2001] also found the highest iron concentrations occurred in early spring, and decreased throughout the summer. They noted that the first pulse of iron in spring corresponds to the timing of the initial shoaling of the 10.5°C isotherm. Although upwelling continues throughout the summer off central California, as it does off Oregon, subsequent upwelling events were not as effective at delivering iron to the surface, either because there was a decrease in the amount of interaction between source waters and shelf sediments or because of a change in the iron content of the source waters. In the current study, considering only the range of $-5 < W_{5d} < 0$, which occurs in both spring and summer, we still find less iron in summer than spring. One interpretation is that for a given upwelling intensity, less iron is delivered to the surface in summer versus spring. It is unclear what would cause this difference; based on the profile data (Figure 5), deep water iron concentrations are if anything higher in summer than spring so there does not appear to have been a decrease in the iron concentration of upwelling source waters. The recent discovery that up to a quarter of the nitrate input to surface waters in this upwelling system is due to cross-isopycnal fluxes [*Hales et al.*, 2005a], as opposed to bulk advection along isopycnals, may be relevant here, in that these fluxes may also be important for iron.
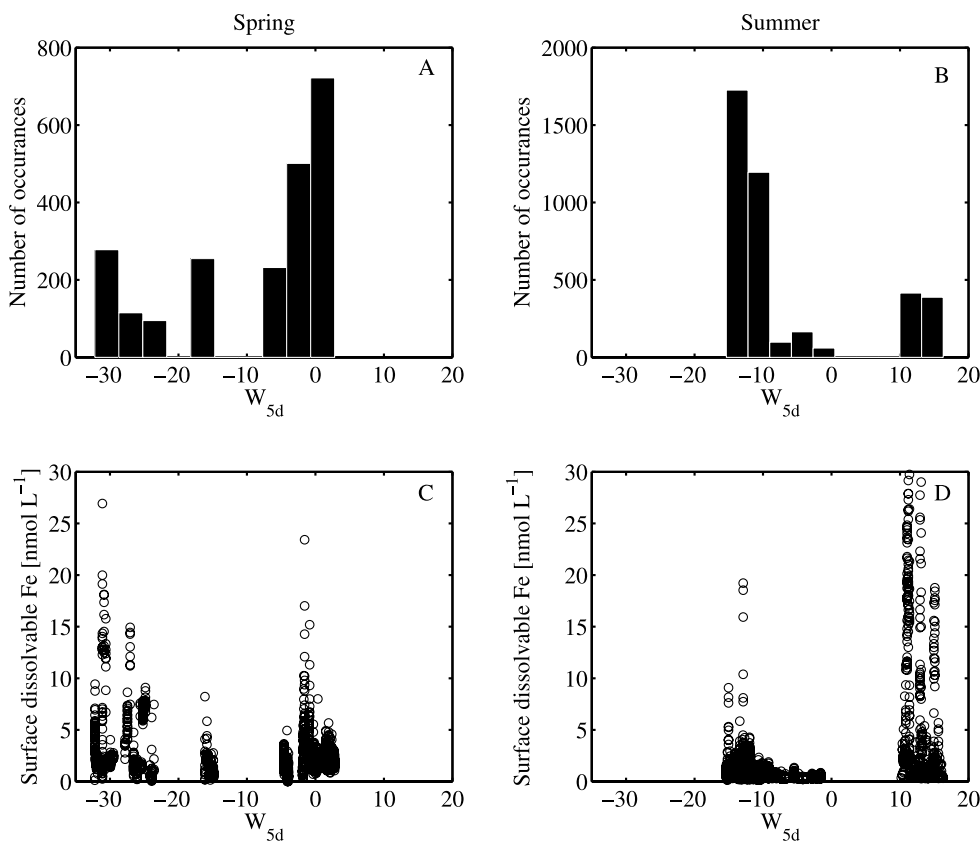
Figure 11. Histograms of the upwelling index, W_{5d} [*Castelao and Barth*, 2005], at times when iron measurements were made, in (a) spring and (b) summer, and (c, d) the corresponding surface dissolvable iron concentrations.

[36] Circulation patterns may also be responsible for some of the spatial variability in iron concentrations. For instance, in the north, along the CH line, the maximum tilting of isotherms occurs close to the coast, while at the CP line the maximum tilting occurs farther offshore, and in deeper water [*Castelao and Barth*, 2005]. This agrees with the observed higher iron concentrations (especially TdFe) at the CH line: to the extent that tilting isotherms represent the pathway of deep water to the surface, one would expect more iron at the surface when the isotherms have a chance to intersect the shelf (i.e., tilt upward in shallow water) before reaching the surface. Another factor to consider is the difference between upwelling that is driven by the curl of the wind stress versus upwelling that is driven by down-coast wind stress and divergence at the coast. The curl-driven upwelling can occur away from the coast [*Huyer*, 1983], and therefore may not interact much with shelf sediments before reaching the surface. This mode of up-welling should produce less iron input than upwelling that occurs in response to Ekman forcing at the coast, where water moves up the shelf in contact with the bottom boundary layer. There is relatively little wind stress curl in the COAST region relative to the southern Oregon coast and California [*Samelson et al.*, 2002].

[37] Total dissolvable iron concentrations also mirror the coastal current remarkably well. Specifically, in spring, TdFe is high nearshore in the north, and a tongue of high TdFe is visible extending offshore near Heceta Bank (be-

tween about 44° and 44.2°N). This pattern is similar to that of the coastal current. Averaged near-surface fields of geo-potential anomaly and 25 m ADCP data show that the coastal jet is close to the coast in the north and moves offshore south of the Bank, separating from the shelf near 43.75°N [*Castelao and Barth*, 2005]. The coastal current may therefore be an effective means of transporting coastal iron offshore. Flow recirculation around the bank at 44°N [*Castelao and Barth*, 2005] may also contribute to low iron concentrations near the coast south of the Bank. This circulation brings offshore (low Fe) waters onto the bank, and is intensified in summer, when it occurs at all depths. The lower iron concentrations at station CP-4 in summer versus spring at all depths (with the exception of the very near-bottom) may be caused by this intrusion of offshore water.

4.4. Meeting Biological Demand for Iron

[38] The COAST site is highly productive during the upwelling season. Biological activity reduces the partial pressure of CO_2 to well below atmospheric [*Hales et al.*, 2005b; *van Geen et al.*, 2000], surface oxygen is 30–50% above saturation [*Hales et al.*, 2003], and nitrate is typically sub micromolar in the surface (Figure 5). In short, phyto-plankton appear able to rapidly consume nutrients and draw down CO_2 in this environment, and iron availability does not appear to be limiting the biological consumption of carbon or nitrogen in this system. In contrast, iron limitation
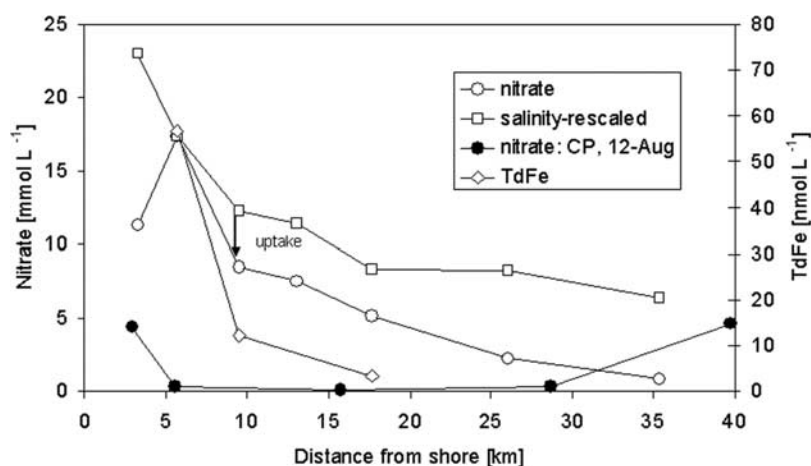
Figure 12. Nitrate and total dissolvable iron (TdFe) concentrations in surface water as a function of distance from shore. Squares denote salinity rescaled to nitrate using CH-2 as a tie point; that is, initial N at CH_n, $CH_nN = [(CH_2N − CH_7N)/(CH_2Sal − CH_7Sal)] × (CH_nSal − CH_2Sal) + CH_2N$. Data are from the surface-most sample from vertical profiles (Figure 4). Data are from the CH line (CH-1 through CH-7) on 10 August unless noted otherwise.

has been identified off the Big Sur coast of central California and the Peru Upwelling/Humboldt Current system [*Bruland et al.*, 2001; *Chase et al.*, 2005; *Hutchins and Bruland*, 1998; *Hutchins et al.*, 2002]. With dissolved iron concentrations in nearshore surface waters of $1-5$ nmol L^{-1} (Figure 6), the COAST region is more akin to the region north of Monterey Bay, where the shelf is wider and iron supply is adequate.

[39] The relative abundance of nitrate and dissolved iron in freshly upwelled water can give an indication of the potential for iron limitation [*Bruland et al.*, 2001]. Elevated nutrient concentrations associated with upwelling exist only transiently in this system. The data of 10 August, on the CH line, are a good example of the system just after upwelling has delivered nutrient-rich water to the nearshore surface. High levels of nitrate and iron are found close to shore, decreasing seaward (Figure 12). At CH-2, 5.6 km from shore, nitrate is 17.4 µmol L^{-1}, silicic acid is 20.2 µmol L^{-1} and phosphate is 1.6 µmol L^{-1}. Total dissolvable Fe is 56.8 nmol L^{-1} and dissolved Fe, 1.6 nmol L^{-1}. At this level of dissolved Fe, assuming it is all readily available, coastal diatoms have a cellular Fe:C ratio of roughly 100 µmol:mol [*Bruland et al.*, 2001; *Sunda and Huntsman*, 1995]. Full assimilation of the 17.4 µmol L^{-1} N by coastal diatoms would therefore require about 11 nmol L^{-1} Fe, more than 6 times what is available. With the 1.6 nmol L^{-1} Fe, taking into account that cellular Fe:C ratios decrease with decreasing Fe availability, only about 7 µmol L^{-1} nitrate could be consumed before diatoms encountered growth rate limitation by Fe [*Bruland et al.*, 2001]. Yet, as discussed above, phytoplankton seem to be regularly able to consume all available nitrate. In this example, although we did not return to sample the same location several days later, we did sample the CP line 2 days later, on 12 August. The low temperature (11.6°C) and high salinity (33.4) of the nearshore surface waters indicates that like the CH line, this area had experienced strong upwelling and nutrient enrichment in the preceding days. By 12 August, however, nitrate concentrations are less than 1 µmol L^{-1} over much of the

shelf (Figure 12). At CP-2, 5.5 km from shore, dissolved and TdFe are 3.1 and 10.2 nmol L^{-1}, respectively, and silicic acid, 0.9 µmol L^{-1}. The almost complete utilization of available nitrate, primarily by diatoms (i.e., the N:Si depletion ratio was roughly unity) had not even severely reduced dissolve Fe concentrations.

[40] The fact that nitrate and silicic acid are consumed completely despite dissolved Fe levels that are apparently too low to support such consumption by coastal diatoms suggests that either coastal diatoms have lower iron requirements than previously believed, or iron from other pools becomes available on the timescale of days, either through dissolution of particulate Fe or through direct utilization of particulate sources [*Nodwell and Price*, 2001]. Many coastal species have Fe:C requirements in the range of $10-60$ µmol:mol [*Maldonado and Price*, 1996; *Schmidt et al.*, 1999]. Average iron requirements of the community would have to be on the order of 15 µmol:mol in order to consume all of the nitrate with the available dissolved iron; this is closer to open ocean iron quotas than those typically associated with coastal species. Alternatively, a fraction of the total dissolvable pool, including colloidal iron, may either be directly accessible to phytoplankton [*Chen et al.*, 2003; *Nodwell and Price*, 2001] or become available through solubilization [*Croot et al.*, 2001]. The relative timing of nutrient uptake, particulate iron solubilization, and loss of particulate iron through sinking is critical. Along the CH line, nutrient concentrations decrease away from shore, partly as a result of mixing with low-nutrient water from offshore and partly due to biological consumption. The decrease in salinity can be used to constrain the loss of iron and nitrate due to mixing alone (Figure 12). In this case most of the nonconservative loss of nitrate (e.g., nitrate consumption) has occurred within 10 km from shore. Total dissolvable Fe is lost very rapidly between 5 and 10 km from shore; the nonconservative loss of TdFe between CH-2 and CH-3 is 28.4 nmol L^{-1}. The majority of this decrease is presumably due to particulate Fe sinking out (rapidly, since it is not found subsurface at CH-3; Figure 4). Yet, in

contrast to TdFe, the concentration of dissolved Fe in the surface actually increases from 1.6 to 4.3 nmol L^{-1} between CH-2 and CH-3. It seems probable that during residence at the surface, some iron is solubilized from particulate sources and can be accessed by phytoplankton. Thus in this system the balance between solubilization, uptake and sinking appears to be tipped in favor of iron becoming available for growth before it sinks from the surface.

[41] In many other regions of the west coast of North America, the balance between iron sources and sinks is not so favorable for phytoplankton growth and nitrate consumption is often less than maximal. Along the Big Sur coast, nitrate concentrations in excess of 10 μmol L^{-1} are regularly observed together with elevated pCO$_2$ (>400 ppm), even after upwelled water has resided at the surface for several days [*Chase et al.*, 2005]. Here, generally less than 2 nmol L^{-1} dissolvable Fe is present in upwelled waters containing $15-20$ μmol L^{-1} nitrate [*Chase et al.*, 2005]. Off Monterey Bay, iron inputs are low enough (on average 1 nmol L^{-1} Fe, 20 km from shore) that some 8 μmol L^{-1} nitrate remains unconsumed 20 km from shore, and even 40 km from shore, on average 5 μmol L^{-1} nitrate is not consumed [*Johnson et al.*, 2001]. The seaward extent of the coastal band of high chlorophyll is noticeably smaller along this part of the coast during summer than it is off Oregon [*Thomas et al.*, 1994]. We hypothesize that iron supply is a key variable influencing the difference in productivity between these coastal upwelling sites. The greater iron supply off Oregon is we believe due to a combination of greater fluvial inputs as well as a difference in the nature of the wind forcing off Oregon. Specifically, if wind relaxation is needed to produce turbid bottom layers [*Lentz and Trowbridge*, 1991; *Pak and Zaneveld*, 1977] then the frequency with which upwelling winds are interrupted by downwelling episodes may be a critical parameter affecting the supply of iron to surface waters in coastal upwelling systems. We note in this context that the variability of wind forcing is greater off Oregon and Washington than it is off California, in the summer and especially in the spring [*Huyer*, 1983].

5. Conclusions

[42] Iron concentrations, particularly total dissolvable iron, are lower in late summer than in spring on the Oregon shelf. This is generally true throughout the water column, except near the bottom, where concentrations in summer are generally higher than in spring. Iron concentrations are highest nearshore in the northern part of the study area, a region where the shelf is relatively narrow and the bathymetry is "simple." This observation is supported by underway measurements in surface waters, discrete measurements in surface waters, and water column profiles.

[43] We used backscatter meters to test the hypothesis that (iron-bearing) particles are transported into surface waters as part of the conveyor circulation classically attributed to upwelling systems. We do not find evidence for this particle transport loop, suggesting that either it does not exist, or that it operates within 15 m of the bottom. However, we do see evidence of downslope transport of particles, and sinking of particles at both the inner and the midshelf, at rates compatible with aggregates of clay and phytoplankton.

These sinking particles may lead to an accumulation of remineralized iron within the benthic boundary layer.

[44] Seasonal changes in iron were likely due to a combination of reduced river influence, increased presence of offshore waters through recirculation on the Bank, and possibly differences in particle mobilization. Summertime biological productivity in this system is not limited by iron. There is enough bioavailable iron to meet the demands of the phytoplankton, which are able to make full use of available nitrate. There is, however, apparently not enough dissolved iron, relative to nitrate, in freshly upwelled water to support full consumption of all the nitrate based on published cellular Fe:C ratios. Presumably additional iron becomes bioavailable while the upwelled water resides at the surface, as excess nitrate is quickly removed though uptake.

References

Allen, J. S., P. A. Newberger, and J. Federiuk (1995), Upwelling circulation on the Oregon continental shelf 1: Response to idealized forcing, *J. Phys. Oceanogr.*, 25, 1843–1866.

Berelson, W., J. McManus, K. Coale, K. Johnson, D. Burdige, T. Kilgore, D. Colodner, F. Chavez, R. Kudela, and J. Boucher (2003), A time series of benthic flux measurements from Monterey Bay, CA, *Cont. Shelf Res.*, 23, 457–481.

Boss, E., and W. S. Pegau (2001), Relationship of light scattering at an angle in the backward direction to the backscattering coefficient, *Appl. Opt.*, 40, 5503–5507.

Bruland, K. W., and E. L. Rue (2001), Iron: Analytical methods for the determination of concentrations and speciation, in *The Biogeochemistry of Iron in Seawater*, edited by K. A. Hunt and D. R. Turner, pp. 255–289, John Wiley, Hoboken, N. J.

Bruland, K. W., E. L. Rue, and G. J. Smith (2001), Iron and macronutrients in California coastal upwelling regimes: Implications for diatom blooms, *Limnol. Oceanogr.*, 46, 1661–1674.

Bunt, J. A. C., P. Larcombe, and C. F. Jago (1999), Quantifying the response of optical backscatter devices and transmissometers to variations in suspended particulate matter, *Cont. Shelf Res.*, 19, 1199–1220.

Castelao, R. M., and J. A. Barth (2005), Coastal ocean response to summer upwelling favorable winds in a region of alongshore bottom topography variations off Oregon, *J. Geophys. Res.*, doi:10.1029/2004JC002409, in press.

Chase, Z., A. van Geen, P. M. Kosro, J. Marra, and P. A. Wheeler (2002), Iron, nutrient, and phytoplankton distributions in Oregon coastal waters, *J. Geophys. Res.*, 107(C10), 3174, doi:10.1029/2001JC000987.

Chase, Z., K. S. Johnson, V. A. Elrod, J. N. Plant, S. E. Fitzwater, L. Pickell, and C. M. Sakamoto (2005), Manganese and iron distributions off central California influenced by upwelling and shelf width, *Mar. Chem.*, 95, 235–254, doi:10.1016/j.marchem.2004.09.006.

Chen, M., R. C. H. Dei, W.-X. Wang, and L. Guo (2003), Marine diatom uptake of iron bound with natural colloids of different origins, *Mar. Chem.*, 81, 177–189.

Croot, P. L., A. R. Bowie, R. D. Frew, M. T. Maldonado, J. A. Hall, K. A. Safi, J. La Roche, P. W. Boyd, and C. S. Law (2001), Retention of dissolved iron and Fe-II in an iron induced Southern Ocean phytoplankton bloom, *Geophys. Res. Lett.*, 28, 3425–3428.

Elrod, V. A., W. M. Berelson, K. H. Coale, and K. S. Johnson (2004), The flux of iron from continental shelf sediments: A missing source for global budgets, *Geophys. Res. Lett.*, 31, L12307, doi:10.1029/2004GL020216.

Fitzwater, S. E., K. S. Johnson, V. A. Elrod, F. P. Chavez, J. Ryan, S. J. Tanner, and R. M. Gordon (2003), Iron and nutrient relationships in upwelled waters of the California coastal system, *Cont. Shelf Res.*, 23, 1523–1544.

Fuhrer, G., G. Tanner, J. Morace, S. McKenzie, and K. Skach (1996), Water quality of the lower Columbia River basin: Analysis of current and historical water-quality data through 1994, *U. S. Geol. Surv. Water Resour. Invest. Rep.*, 95-4294, 168 pp.

Fung, I. Y., S. K. Meyn, I. Tegen, S. C. Doney, J. G. John, and J. K. B. Bishop (2000), Iron supply and demand in the upper ocean, *Global Biogeochem. Cycles*, 14, 281–295.

Gordon, L. I., J. J. C. Jennings, A. A. Ross, and J. M. Krest (1994), A suggested protocol for continuous flow analysis of seawater nutrients (phosphate, nitrate, nitrite, and silicic acid) in the WOCE Hydrographic Program and the Joint Global Ocean Fluxes Study, office report, WOCE Hydrograph. Prog., Woods Hole, Mass.

Gran, H. H. (1931), On the conditions for the production of plankton in the sea, *Rapp. Proc. Verb. Cons. Int. Explor. Mer.*, 75, 37–46.

Hales, B., L. Karp-Boss, J. Moum, P. Wheeler, P. Covert, and L. Bandstra (2003), Off-shelf export of POC from the Oregon coast: Implications for uptake of atmospheric CO₂, *Eos Trans. AGU*, 84(52), Ocean Sci. Meet. Suppl., Abstract OS51L-02.

Hales, B., J. N. Moum, P. A. Covert, and A. Perlin (2005a), Irreversible nitrate fluxes due to turbulent mixing in a coastal upwelling system, *J. Geophys. Res.*, doi:10.1029/2004JC002685, in press.

Hales, B., T. Takahashi, and L. Bandstra (2005b), Atmospheric CO₂ uptake by a coastal upwelling system, *Global Biogeochem. Cycles*, 19, GB1009, doi:10.1029/2004GB002295.

Hamm, C. E. (2002), Interactive aggregation and sedimentation of diatoms and clay-sized lithogenic material, *Limnol. Oceanogr.*, 47, 1790–1795.

Hickey, B. M., and N. S. Banas (2003), Oceanography of the U.S. Pacific Northwest coastal ocean and estuaries with application to coastal ecology, *Estuaries*, 26, 1010–1031.

Huettel, M., W. Ziebis, S. Forster, and G. W. Luther (1998), Advective transport affecting metal and nutrient distributions and interfacial fluxes in permeable sediments, *Geochim. Cosmochim. Acta*, 62, 613–631.

Hutchins, D. A., and K. W. Bruland (1998), Iron-limited diatom growth and Si:N uptake ratios in a coastal upwelling regime, *Nature*, 393, 561–564.

Hutchins, D. A., et al. (2002), Phytoplankton iron limitation in the Humboldt Current and Peru Upwelling, *Limnol. Oceanogr.*, 47, 997–1011.

Huyer, A. (1983), Coastal upwelling in the California Current system, *Prog. Oceanogr.*, 12, 259–284.

Huyer, A., R. L. Smith, and J. Fleischbein (2002), The coastal ocean off Oregon and northern California during the 1997–98 El Niño, *Prog. Oceanogr.*, 54, 311–341.

Johnson, K. S., F. P. Chavez, and G. E. Friederich (1999), Continental-shelf sediment as a primary source of iron for coastal phytoplankton, *Nature*, 398, 697–700.

Johnson, K. S., F. P. Chavez, V. A. Elrod, S. E. Fitzwater, J. T. Pennington, K. R. Buck, and P. M. Walz (2001), The annual cycle of iron and the biological response in central California coastal waters, *Geophys. Res. Lett.*, 28, 1247–1251.

Kulm, L. D., R. C. Roush, J. C. Harlett, R. H. Neudeck, D. C. Chambers, and E. J. Runge (1975), Oregon continental shelf sedimentation: Interrelationships of facies distribution and sedimentary processes, *J. Geol.*, 83, 145–175.

Lenes, J. M., B. P. Darrow, C. Cattrall, C. A. Heil, M. Callahan, G. A. Vargo, and R. H. Byrne (2001), Iron fertilization and the *Trichodesmium* response on the west Florida shelf, *Limnol. Oceanogr.*, 46, 1261–1277.

Lentz, S. J., and J. H. Trowbridge (1991), The bottom boundary-layer over the northern California shelf, *J. Phys. Oceanogr.*, 21, 1186–1201.

Lohan, M. C., and K. W. Bruland (2004), Importance of vertical mixing for additional sources of nitrate and iron to surface waters of the Columbia River plume: Implications for biology, *Eos Trans. AGU*, 85(47), Fall Meet. Suppl., Abstract OS11B-03.

Maldonado, M. T., and N. M. Price (1996), Influence of N substrate on Fe requirements of marine centric diatoms, *Mar. Ecol. Prog. Ser.*, 141, 161–172.

Maldonado, M. T., M. P. Hughes, E. L. Rue, and M. L. Wells (2002), The effect of Fe and Cu on growth and domoic acid production by *Pseudonitzschia multiseries* and *Pseudo-nitzschia australis*, *Limnol. Oceanogr.*, 47, 515–526.

Measures, C. I., J. Yuan, and J. A. Resing (1995), Determination of iron in seawater by flow injection analysis using in-line preconcentration and spectrophotometric detection, *Mar. Chem.*, 50, 3–12.

Nodwell, L. M., and N. M. Price (2001), Direct use of inorganic colloidal iron by marine mixotrophic phytoplankton, *Limnol. Oceanogr.*, 46, 765–777.

Pak, H., and J. R. V. Zaneveld (1977), Bottom nepheloid layers and bottom mixed layers observed on the continental-shelf off Oregon, *J. Geophys. Res.*, 82, 3921–3931.

Perlin, A., J. N. Moum, and J. Klymak (2005), Response of the bottom boundary layer over a sloping shelf to variations in alongshore wind, *J. Geophys. Res.*, doi:10.1029/2004JC002500, in press.

Samelson, R., P. Barbour, J. Barth, S. Bielli, T. Boyd, D. Chelton, P. Kosro, M. D. Levine, and E. Skyllingstad (2002), Wind stress forcing of the Oregon coastal ocean during the 1999 upwelling season, *J. Geophys. Res.*, 107(C5), 3034, doi:10.1029/2001JC000900.

Schmidt, M. A., Y. Zhang, and D. A. Hutchins (1999), Assimilation of Fe and carbon by marine copepods from Fe-limited and Fe-replete diatom prey, *J. Plankton Res.*, 21, 1753–1764.

Smith, W. O., Jr., G. W. Heburn, R. T. Barber, and J. J. Obrien (1983), Regulation of phytoplankton communities by physical processes in upwelling ecosystems, *J. Mar. Res.*, 41, 539–556.

Sunda, W. G., and S. A. Huntsman (1995), Iron uptake and growth limitation in oceanic and coastal phytoplankton, *Mar. Chem.*, 50, 189–206.

Takesue, R. K., and A. van Geen (2002), Nearshore circulation during upwelling inferred from the distribution of dissolved cadmium off the Oregon coast, *Limnol. Oceanogr.*, 47, 176–185.

Thomas, A. C., F. Huang, P. T. Strub, and C. James (1994), Comparison of the seasonal and interannual variability of phytoplankton pigment concentrations in the Peru and California Current systems, *J. Geophys. Res.*, 99, 7355–7370.

van Geen, A., R. K. Takesue, J. Goddard, T. Takahashi, J. A. Barth, and R. L. Smith (2000), Carbon and nutrient dynamics during coastal upwelling off Cape Blanco, Oregon, *Deep Sea Res., Part II*, 47, 975–1002.

van Ierland, E. T., and L. Peperzak (1984), Separation of marine seston and density determination of marine diatoms by density gradient determination, *J. Plankton Res.*, 6, 29–44.

Vink, S., E. A. Boyle, C. I. Measures, and J. Yuan (2000), Automated high resolution determination of the trace elements iron and aluminum in the surface ocean using a towed fish coupled to flow injection analysis, *Deep Sea Res., Part I*, 47, 1141–1156.

_____

Z. Chase, T. Cowles, and B. Hales, College of Oceanic and Atmospheric Sciences, Oregon State University, Corvallis, OR 97331-5503, USA. (zanna@coas.oregonstate.edu; tjc@coas.oregonstate.edu; bhales@coas.oregonstate.edu)

R. Schwartz and A. van Geen, Lamont Doherty Earth Observatory of Columbia University, Palisades, NY 10964, USA. (roseanne@ldeo.columbia.edu; avangeen@coas.oregonstate.edu)